

EFFECT OF TE AND SB DOPING ON THE ELECTRICAL PROPERTIES OF $\text{Li}_{0.25}\text{La}_{0.25}\text{NbO}_3$ CERAMICS

*YAZHOU KONG, SHIHANG HU, GUANG HU, WEIWEI HU, #KAILONG ZHANG, JIADONG ZHANG, KUN HONG

National & Local Joint Engineering Research Center for Mineral Salt Deep Utilization, Faculty of Chemical Engineering, Huaiyin Institute of Technology, Huaian 223003, P. R. China

#E-mail: kongyazhou@hyit.edu.cn; zkl045@mail.ustc.edu.cn

Submitted June 19, 2023; accepted July 27, 2023

Keywords: Solid electrolyte, Perovskite, Dope, Conductivity

The effects of Te and Sb doping on the structure and conductivity of the $\text{Li}_{0.25}\text{La}_{0.25}\text{NbO}_3$ (LLNO) solid electrolyte were comparatively studied. Te and Sb doped LLNO with a defect perovskite structure was prepared via a solid-state reaction method. The moderate doping of Te and Sb improves the conductivity of LLNO. The grain conductivity and grain boundary conductivity of the LLNO ceramics was distinguished through the equivalent circuit fitting method. With the same doping amount, the Te doped samples exhibit higher grain and total conductivity than the Sb doped samples. $\text{Li}_{0.25}\text{La}_{0.25}\text{Nb}_{0.95}\text{Te}_{0.05}\text{O}_3$ has the highest total conductivity of $4.04 \times 10^{-5} \text{ S}\cdot\text{cm}^{-1}$ at 30 °C, which is two times higher than the pure LLNO solid electrolyte. The DC-polarization characterization indicated that $\text{Li}_{0.25}\text{La}_{0.25}\text{Nb}_{0.95}\text{Te}_{0.05}\text{O}_3$ and $\text{Li}_{0.25}\text{La}_{0.25}\text{Nb}_{0.95}\text{Sb}_{0.05}\text{O}_3$ have an extremely low electronic conductivity. The LLNO ceramics doped with Te and Sb are still solid electrolyte materials with lithium-ion transportation properties.

INTRODUCTION

Devices based on solid state ionics [1] have been widely used for metallurgical sensors, solid batteries, Li-metal extraction from the sea and electrochromic glazing. Research and development into high-performance solid electrolytes is an important direction of solid state ionics [2]. $\text{Li}_{0.25}\text{La}_{0.25}\text{NbO}_3$ (LLNO) is a typical solid electrolyte with an ABO_3 -type defect perovskite structure [3]. $\text{Li}_{0.25}\text{La}_{0.25}\text{NbO}_3$ (LLNO) exhibits Li^+ conducting properties at room temperature due to the presence of A-site vacancy [4]. Moreover, LLNO is possibly a stable Li^+ conducting solid electrolytes in contact with metal lithium [5].

However, the room temperature conductivity of $\sim 1.02 \times 10^{-5} \text{ S}\cdot\text{cm}^{-1}$ for LLNO cannot meet the application requirements. Fujiwara [6] et al. prepared single crystal $\text{Li}_x\text{La}_{(1-x)/3}\text{NbO}_3$ solid electrolytes with a maximum room temperature conductivity of $1.9 \times 10^{-4} \text{ S}\cdot\text{cm}^{-1}$ at $x = 0.08$. This is the highest conductivity for LLNO reported to date. However, the preparation process of a single crystal is complicated. Kawakami [7] et al. reported on a lattice expansion strategy to improve the conductivity for LLNO. Part of the Li^+ and La^{3+} with a small ionic radius were equally substituted by Sr^{2+} with a large ionic radius and the perovskite lattice was expanded, which is beneficial to Li^+ migration. Belous [8] et al. put forward the partial A-site disordering strategy to improve the conductivity of LLNO. The partial isovalent substitution

of Na^+ for Li^+ in LLNO resulted in the partial disordering for the perovskite structure. This strategy improved the room temperature conductivity of the LLNO solid electrolyte significantly. On the other hand, sodium substitution for lithium increased the lattice parameters and cell volume of LLNO, which is also beneficial for the Li^+ migration. To sum up, doping is an effective way to improve the electrical properties of LLNO ceramics.

In this study, the effect of Te and Sb doping on the structure and conductivity of LLNO were comparatively studied. The Te and Sb doped LLNO ceramic electrolytes was prepared via the solid-state reaction method. The structure, microstructure and electrical properties of the LLNO-based ceramic solid electrolytes were investigated by X-ray diffraction (XRD), Scanning electron microscopy (SEM), AC-impedance and DC-polarization.

EXPERIMENTAL

Te and Sb doped $\text{Li}_{0.25}\text{La}_{0.25}\text{NbO}_3$ (LLNO) ceramic electrolytes were prepared via the solid-state reaction method. Li_2CO_3 (99.9 %, Kelong Chemical Co.), TeO_2 (99.9 %, Kelong Chemical Co.), La_2O_3 (99.8 %, Guoyao Chemical Co.), Nb_2O_5 (99.5 %, Guoyao Co.) and Sb_2O_5 (99.5 %, Guoyao Co.) were used as the raw materials. The compositions of the target compounds are $\text{Li}_{0.25}\text{La}_{0.25}\text{NbO}_3$ (LLNO), $\text{Li}_{0.25}\text{La}_{0.25}\text{Nb}_{0.95}\text{Te}_{0.05}\text{O}_3$

(LLNO-T005), $\text{Li}_{0.25}\text{La}_{0.25}\text{Nb}_{0.9}\text{Te}_{0.1}\text{O}_3$ (LLNO-T01), $\text{Li}_{0.25}\text{La}_{0.25}\text{Nb}_{0.95}\text{Sb}_{0.05}\text{O}_3$ (LLNO-S005) and $\text{Li}_{0.25}\text{La}_{0.25}\text{Nb}_{0.9}\text{Sb}_{0.1}\text{O}_3$ (LLNO-S01). The reagents were mixed in the desired molar ratio via ball-milling. The mixture was calcined at 900 °C for 12 h and then pelletised under 10 MPa. All the ceramic pellets were sintered at 1100 °C for 12 h before air quenching.

The phase composition of the pellets was obtained using X-ray diffraction (XRD) on a Rigaku-2500 device. The cross-section microstructure of pellets was characterized via a scanning electron microscope (SEM) on an S-3000N device. The conductivity of the pellet was determined via AC-impedance in the frequency range from 1 MHz to 0.1 Hz at 10, 30, 60, 80, 100 and 120 °C. The electronic conductivity of the samples was estimated using DC-polarization with a potential of 4 V for 8000 s at 30 °C on a CHI660E device. An Ag-based blocking electrode was used for both the AC-impedance and DC-polarization test.

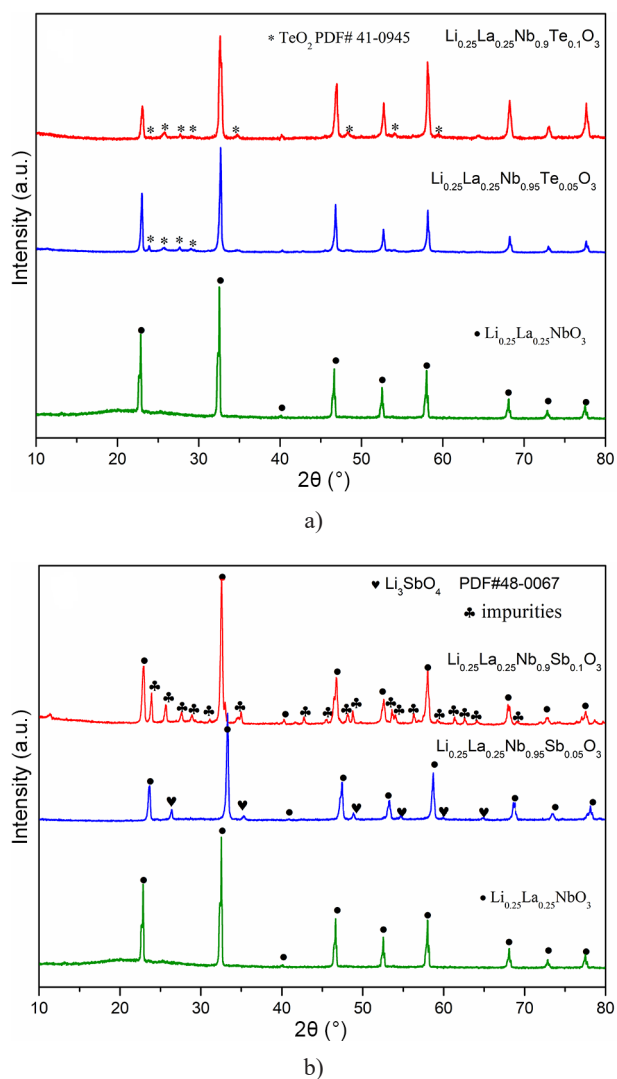


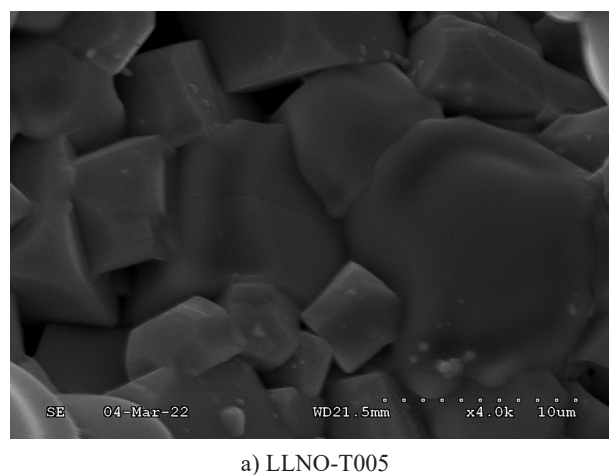
Figure 1. XRD patterns of the sintered ceramic pellets: a) Te-doped samples, b) Sb-doped samples.

RESULTS AND DISCUSSION

Figure 1a shows the XRD patterns of the LLNO and Te-doped LLNO samples. The as-sintered pure LLNO presents a single phase with a perovskite structure, the space group is Pmmm. TeO_2 impurities were detected in both LLNO-T005 and LLNO-T01. The TeO_2 impurity content in LLNO-T01 was higher than that in LLNO-T005. The ion radius of Te^{6+} (0.56 Å) is lower than Nb^{5+} (0.64 Å). The main diffraction peaks of both LLNO-T005 and LLNO-T01 shifted toward a high angle compared to the pure LLNO. This result indicates that a certain amount of Te^{6+} was successfully doped into the Nb^{5+} site in both LLNO-T005 and LLNO-T01. However, the main diffraction peaks of LLNO-T01 are localised in the same angle with LLNO-T005. Not all the Te^{6+} was doped into the LLNO ceramic. The excess Te^{6+} formed an impurity phase.

Figure 1b shows the XRD patterns of the Sb-doped LLNO. The main phase of both LLNO-Sb005 and LLNO-Sb01 correspond to the perovskite structure. The main diffraction peaks of LLNO-Sb005 tended toward a high angle compared to the pure LLNO due to the fact that the ion radius of Sb^{5+} (0.60 Å) is lower than Nb^{5+} (0.64 Å). Li_3SbO_4 impurities were found in LLNO-Sb005. A great deal of impurities were detected in LLNO-Sb01. When the doping amount of Sb increased, serious side reactions occurred, Sb preferred to form impurities rather than being doped into the lattice of LLNO.

Figure 2 shows the fractured SEM images of the sintered ceramic pellets. The grains are rectangular in shape. It can be observed that the grains are in good contact with the adjacent grains. The grain-boundary can be clearly observed. The average grain size of all the samples is similar, approximately 5 - 10 μm. The density of the LLNO and the doped samples was determined by the Archimedes method. The density of LLNO,



a) LLNO-T005

Figure 2. SEM images of: a) LLNO-T005. (Continue on next page)

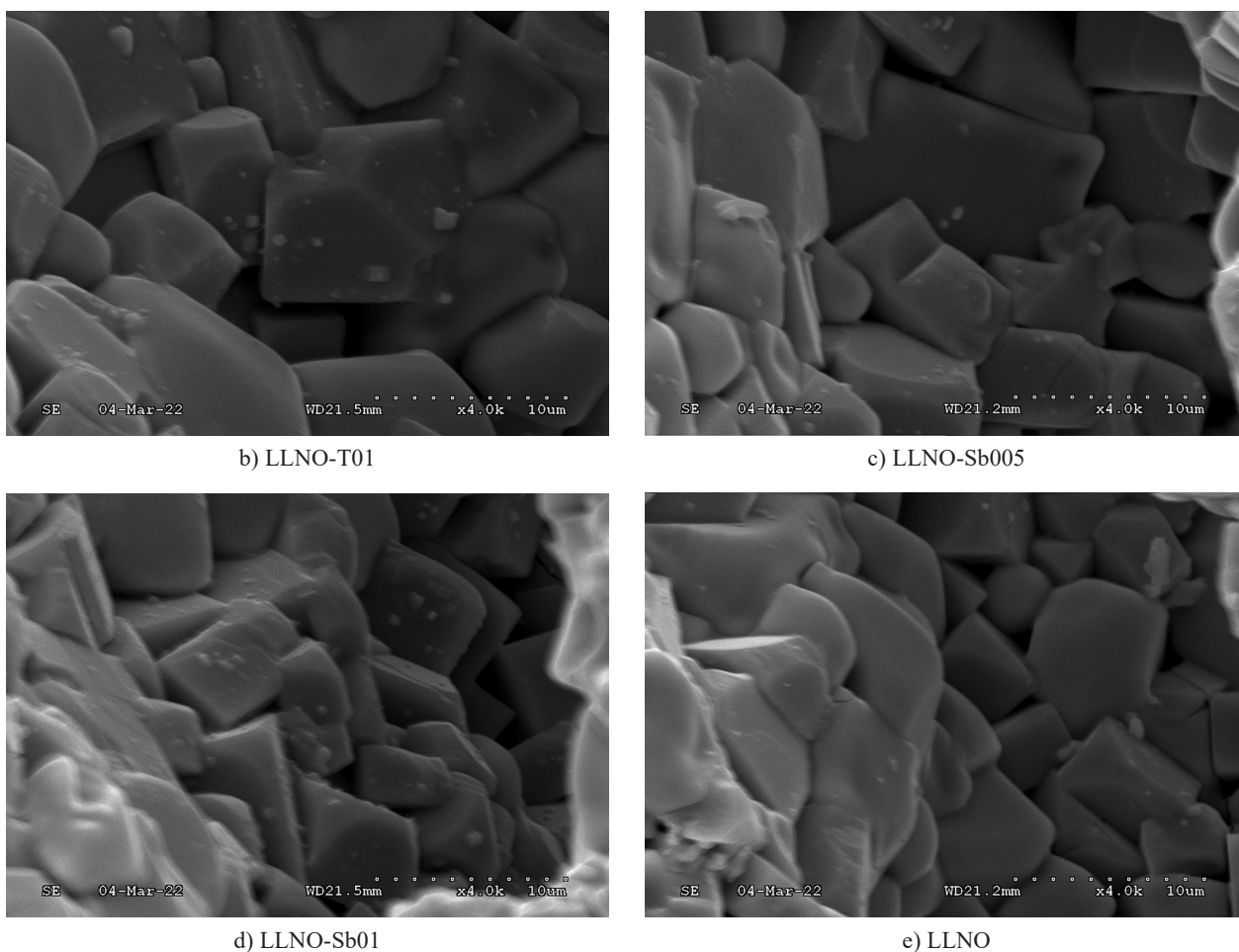


Figure 2. SEM images of: b) LLNO-T01, c) LLNO-Sb005, d) LLNO-Sb01 and e) LLNO.

LLNO-T005, LLNO-T01, LLNO-Sb005 and LLNO-Sb01 was 4.39, 4.41, 4.46, 4.43 and 4.49 $\text{g}\cdot\text{cm}^{-3}$, respectively. All the doping samples have a little higher density than the pure LLNO. This may be attributed to the low melting point of TeO_2 (melting point of 733 °C) and Sb_2O_5 (melting point of 300 °C), which were added into the raw material and can act as sintering aids.

Figure 3 shows the Nyquist plots of the samples at 30 °C. The semicircle observed at the high frequency region represents the grain resistance of the ceramic. Meanwhile, the semicircle observed at the low frequency region represents the grain-boundary resistance of the ceramic. The resistance value is the X-axis intercept of the corresponding semicircle. The overall resistance for

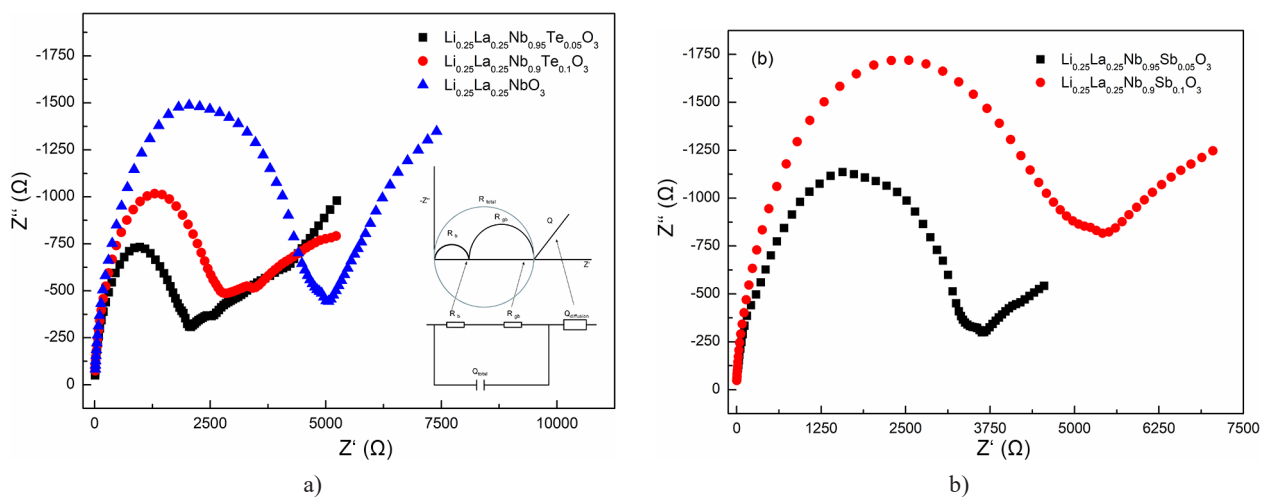


Figure 3. AC-impedance spectra of the: a) Te-doped samples and b) Sb-doped samples.

the ceramic is the sum of the grain and grain-boundary resistance. As can be seen in Figure 3a, LLNO-T005 has the minimum total resistance. A certain amount of Te^{6+} doping for the Nb^{5+} site reduces the total resistance of the samples. A further increase in the Te doping content led to an increase in the total resistance. The total resistance of LLNO-Sb005 was slightly smaller than the pure LLNO, as shown in Figure 3b. However, LLNO-Sb01 had the highest total resistance among all the samples.

The grain resistance and grain boundary resistance of the LLNO ceramics was distinguished through the equivalent circuit fitting method. The grain and grain-boundary conductivity of each sample were calculated and are listed in Table 1. The grain conductivity of the samples increased after the Te doping. LLNO-T005 exhibits the highest grain conductivity of $5.06 \times 10^{-5} \text{ S}\cdot\text{cm}^{-1}$ at 30 °C. A further increase in the Te doping content led to a decrease in the grain conductivity. All the Te doped samples have lower grain-boundary conductivity than that of the pure LLNO. A small quantity of Te doping is beneficial in increasing the grain conductivity. For the Sb doped samples, LLNO-S005 has a higher grain conductivity than the pure LLNO, but LLNO-S01 presented with low grain conductivity, low grain-boundary conductivity, and low total conductivity. The Sb doping cannot improve the conductivity of LLNO effectively, and even had a negative effect.

The aliovalent doping of Te^{6+} for Nb^{5+} produced vacancies, which is beneficial to Li^+ conduction in

the grains. The Sb doping did not have this effect. LLNO-T005 exhibits the highest total conductivity of $4.04 \times 10^{-5} \text{ S}\cdot\text{cm}^{-1}$ at 30 °C, which is two times higher than the pure LLNO ceramic. With the same amount of doping, the Te doped samples have high grain and total conductivity. However, the grain-boundary conductivity of the Sb doped samples was higher than Te doped samples. This may be attributed to the low melting point of Sb_2O_5 (300 °C). Sb_2O_5 played the role of a sintering aid rather than being doped into the LLNO during the sintering, which is beneficial to improving the grain boundary conductivity. Furthermore, excessive impurities are also one of the important reasons for the low conductivity of the Sb doped samples.

The activation energy (E_a) for the total conductivity of all the samples were estimated from the Arrhenius plots shown in Figure 4 via the Arrhenius equation. The activation energy of each sample is listed in Table 1. The activation energy determined from the Arrhenius equation is 0.411, 0.322, 0.379, 0.371 and 0.412 eV for LLNO, LLNO-T005, LLNO-T01, LLNO-S005 and LLNO-S01, respectively. LLNO-T005 has a low activation energy. The vacancy created by the Te doping provided more lithium-ion migration pathways. The Te doping is beneficial to the Li^+ transportation in the LLNO perovskite structure.

The steady current shown in Figure 5 was attributed to the electronic conduction in the LLNO-based ceramic pellet. The steady current of LLNO-T005 and

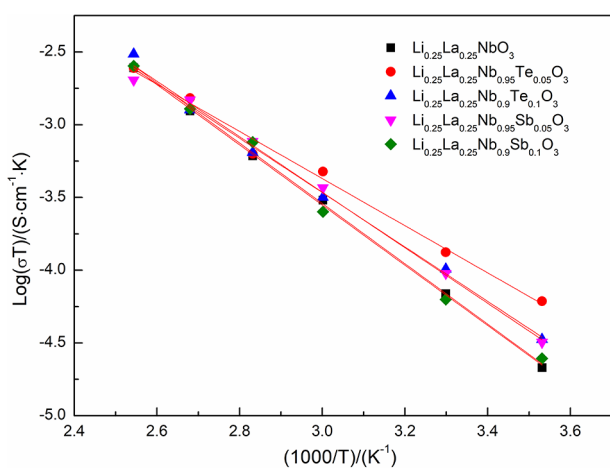


Figure 4. Arrhenius plots of the total ionic conductivity for the samples.

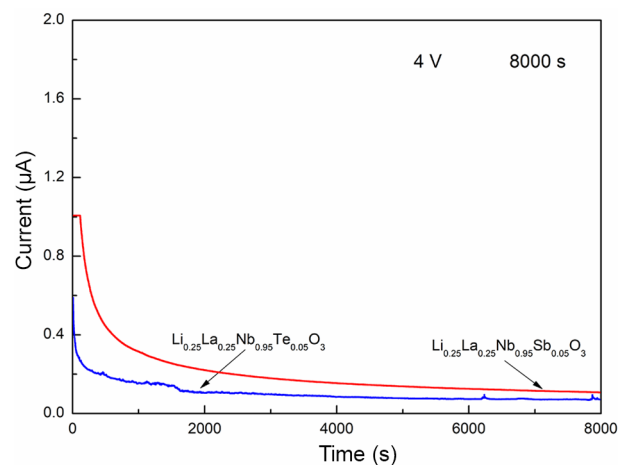


Figure 5. DC-polarisation current as a function of the polarisation time at 30 °C for LLNO-T005 and LLNO-S005.

Table 1. Conductivity and activation energy of the Te and Sb doped LLNO ceramics.

Samples	Grain conductivity ($\text{S}\cdot\text{cm}^{-1}$)	Grain boundary conductivity ($\text{S}\cdot\text{cm}^{-1}$)	Total conductivity ($\text{S}\cdot\text{cm}^{-1}$)	Activation energy (eV)
LLNO	2.18×10^{-5}	4.76×10^{-4}	2.09×10^{-5}	0.411
LLNO-T005	5.06×10^{-5}	1.99×10^{-4}	4.04×10^{-5}	0.322
LLNO-T01	3.72×10^{-5}	1.83×10^{-4}	3.09×10^{-5}	0.379
LLNO-S005	3.08×10^{-5}	4.44×10^{-4}	2.88×10^{-5}	0.371
LLNO-S01	2.08×10^{-5}	2.17×10^{-4}	1.91×10^{-5}	0.412

LLNO-S005 was 0.09 μA and 0.17 μA , respectively. The electronic conductivity of LLNO-T005 and LLNO-S005 was determined to be $2.31 \times 10^{-9} \text{ S}\cdot\text{cm}^{-1}$ and $4.47 \times 10^{-9} \text{ S}\cdot\text{cm}^{-1}$, respectively. The electronic conductivity of LLNO-T005 and LLNO-S005 is 4 orders of magnitude lower than that of the corresponding ionic conductivity. The electronic conductivity of both LLNO-T005 and LLNO-S005 was negligible. Therefore, lithium-ion transportation occupies an absolute dominant position in these samples.

CONCLUSIONS

The structure and conductivity properties of the defect-perovskite type $\text{Li}_{0.23}\text{La}_{0.25}\text{NbO}_3$ ceramic solid electrolyte created by Te and Sb doping were comparatively studied. The main diffraction peaks of LLNO and all the doped samples corresponded to a perovskite structure. TeO_2 impurities were detected in both LLNO-T005 and LLNO-T01. A great deal of impurities were detected in LLNO-Sb01. With the same amount of doping, the Te doped samples had a high grain and total conductivity. LLNO-T005 exhibits the highest total conductivity of $4.04 \times 10^{-5} \text{ S}\cdot\text{cm}^{-1}$ at 30 $^\circ\text{C}$, which is two times higher than the pure LLNO ceramic. The aliovalent ion doping of Te^{6+} for Nb^{5+} produced vacancies, which are beneficial to Li^+ conduction in ceramics. The vacancy created by the Te doping provided more lithium-ion migration pathways. The electronic conductivity of LLNO-T005 and LLNO-S005 was 4 orders of magnitude lower than the corresponding ionic conductivity. LLNO-T005 and LLNO-S005 can be considered as solid electrolytes.

Acknowledgements

This work was supported by the Research Start-up Fund of the Huaiyin Institute of Technology (Z301B20574, Z301B20514, Z301B19582), the fund of the National & Local Joint Engineering Research Center for Mineral Salt Deep Utilization (SF202206) and the Foundation of Key Laboratory for Palygorskite Science and Applied Technology of Jiangsu Province (HPZ202201).

REFERENCES

1. Wu F., Liu L., Wang S., Xu J., Lu P., Yan W., Li H. (2022): Solid state ionics – Selected topics and new directions. *Progress in Materials Science*, 126, 100921. Doi: 10.1016/j.pmatsci.2022.100921
2. Lu X. (2021): Enhanced conductivity of perovskite lithium-ion conductors under the influence of nano-cellulose fibres. *Ceramics – Silikaty*, 65(1), 107–112. Doi: 10.13168/cs.2021.0008
3. Jiménez R., Díez V., Sanz J., Kobylanska S. D., V'yunov O. I., Belous A. G. (2015): Evidence for changes on the lithium conduction dimensionality of $\text{Li}_{0.5-y}\text{Na}_y\text{La}_{0.5}\text{Nb}_2\text{O}_6$ ($0 \leq y \leq 0.5$) perovskites. *RSC Advances*, 5(35), 27912–27921. Doi: 10.1039/C5RA02505B
4. Hu X., Kobayashi S., Ikuhara Y. H., Fisher C. A. J., Fujiwara Y., Hoshikawa K., Ikuhara Y. (2017): Atomic scale imaging of structural variations in $\text{La}_{(1-x)}\text{Li}_x\text{NbO}_3$ ($0 \leq x \leq 0.13$) solid electrolytes. *Acta Materialia*, 123, 167–176. Doi: 10.1016/j.actamat.2016.10.025
5. Nadiri A., Le Flem G., Delmas C. (1988): Lithium intercalation in perovskite-type phases (Ln = La, Nd). *Journal of Solid State Chemistry*, 73(2), 338–347. Doi: 10.1016/0022-4596(88)90118-1
6. Fujiwara Y., Hoshikawa K., Kohama K. (2016): Growth of solid electrolyte $\text{Li}_x\text{La}_{(1-x)/3}\text{NbO}_3$ single crystals by the directional solidification method. *Journal of Crystal Growth*, 433, 48–53. Doi: 10.1016/j.jcrysgro.2015.09.033
7. Kawakami Y., Fukuda M., Ikuta H., Wakihara M. (1998): Ionic conduction of lithium for perovskite type compounds, $(\text{Li}_{0.05}\text{La}_{0.317})_{1-x}\text{Sr}_{0.5}\text{NbO}_3$, $(\text{Li}_{0.1}\text{La}_{0.3})_{1-x}\text{Sr}_{0.5}\text{NbO}_3$ and $(\text{Li}_{0.25}\text{La}_{0.25})_{1-x}\text{M}_{0.5}\text{NbO}_3$ (M=Ca and Sr). *Solid State Ionics*, 110(3–4), 187–192. Doi: 10.1016/S0167-2738(98)00131-3
8. Belous A., Pashkova E., Gavrilenko O., V'yunov O., Kovalenko L. (2003): Solid electrolytes based on lithium-containing lanthanum metaniobates and metatantalates with defect-perovskite structure. *Ionics*, 9(1–2), 21–27. Doi: 10.1007/BF02376532